

## Synthesis and Characterization of Ultrafine and Porous Structure of Magnesium Ferrite Nanospheres

Research Article

M. Penchal Reddy<sup>1\*</sup>, X. B. Zhou<sup>1</sup>, Q. Huang<sup>1</sup>, R. Ramakrishna Reddy<sup>2</sup><sup>1</sup>Ningbo Institute of Materials Technology and Engineering (NIMTE), Chinese Academy of Sciences (CAS), Ningbo 315201, Zhejiang, RP China.<sup>2</sup>Department of Physics, Sri Krishnadevaraya University, Anantapur 515 001, India.

## Abstract

Porous sphere-shaped magnesium ( $\text{MgFe}_2\text{O}_4$ ) spinel ferrite particles were synthesized with high yields, crystallinity and purity through an easy, quick, reproducible and low-temperature hydrothermal synthesis route starting from an aqueous suspension of coprecipitated metal oxalates. The structural and morphological properties of the prepared materials were characterized by X-ray diffraction, scanning electron microscopy, transmission electron microscopy, energy-dispersive X-ray spectroscopy, infrared spectroscopy and  $\text{N}_2$  adsorption-desorption measurement. Results show that the obtained  $\text{MgFe}_2\text{O}_4$  particles are nearly spherical in shape and about 100-250 nm in mean diameter. Every magnetic microsphere is made of many ultrafine  $\text{MgFe}_2\text{O}_4$  nanoparticles and porous in structure. The obtained sphere-shaped products exhibited a saturation magnetization of 70.25 emu/g and a coercivity of 326.41 Oe at room temperature.

**Keywords:**  $\text{MgFe}_2\text{O}_4$  Nanospheres; Hydrothermal method; Porous structure; Magnetic properties; Electron microscopy

**\*Corresponding Author:**

M. Penchal Reddy,  
Ningbo Institute of Materials Technology and Engineering (NIMTE),  
Chinese Academy of Sciences (CAS), Ningbo 315201, Zhejiang, RP  
China.

Tel.: + 86-13867877545

E-mail: reddy@nimte.ac.cn

**Received:** November 23, 2014**Accepted:** November 28, 2014**Published:** December 11, 2014

**Citation:** M. Penchal Reddy, X. B. Zhou, Q. Huang, R. Ramakrishna Reddy (2014) Synthesis and Characterization of Ultrafine and Porous Structure of Magnesium Ferrite Nanospheres. *Int J Nano Stud Technol.* 3(6), 72-77. doi: <http://dx.doi.org/10.19070/2167-8685-1400014>

**Copyright:** M. Penchal Reddy<sup>©</sup> 2014 This is an open-access article distributed under the terms of the Creative Commons Attribution License, which permits unrestricted use, distribution and reproduction in any medium, provided the original author and source are credited.

**Introduction**

Functional magnetic materials, such as transition metal oxides with spinel structure  $\text{MFe}_2\text{O}_4$  (M=Mg, Mn, Fe, Co, Ni, Zn, etc.) are one family of the most important materials in advanced technology [1,2]. As an important part of nanomaterials, nanomagnetic materials have attracted considerable attention due to their utilizations in the magnetic field sensor, bio-sensors, magnetic-storage media, catalysis, optics, sensors and drug-delivery carriers, and so on [3-9]. However, the magnetic properties of nanoparticles strongly depend on the synthesis conditions, particle size, shape and composition. Therefore, the ability to manipulate the shape and size of nanomaterials is crucial to determine their magnetic properties

and achieve the scientific and technological needs. Hence, it is desirable to develop strategies for morphology-controlled synthesis of nanosized spinel ferrites.

Currently, different morphologies of spinel ferrites have been reported, including nanospheres [9], nanorods [10,11], hollow tubes [12,13], spindle-shaped spinel [14] and nanowires [15,16]. There are few reports on porous sphere-shaped ferrites. Porous-structured ferrites should perform even more effectively in catalysis, adsorption and wave absorption because of their porous framework [17,18].

Among the family of ferrite materials, magnesium ferrite ( $\text{MgFe}_2\text{O}_4$ ) is one of the most important ferrites. It has a cubic structure of normal spinel-type and is a soft magnetic n-type semiconducting material, which finds a number of applications in heterogeneous catalysis, adsorption, sensors, and in magnetic technologies [19]. To date, a variety of synthetic approaches, including solvothermal method [9], solid-state reaction [20,21] polymer calcination approach [22], pulsed laser deposition technique [23] and co-precipitation method [24] have been reported to prepare  $\text{MgFe}_2\text{O}_4$  nanoparticles. However, these reports reveal that high temperature treatment, long time consuming, and complex procedures are generally required for effective synthesis of such functional materials. Therefore, developing simpler and environmentally benign methods is technically important and desired.

In this study, porous sphere-shaped  $\text{MgFe}_2\text{O}_4$  particles were fabricated using low-temperature hydrothermal method. Ethylene glycol (EG) and poly-ethylene glycol (PEG) were used as the solvent and so template, respectively. Magnesium chloride ( $\text{MgCl}_2 \cdot 6\text{H}_2\text{O}$ ) and ferric chloride ( $\text{FeCl}_3 \cdot 6\text{H}_2\text{O}$ ) were used as cation sources in the reaction system. The as-prepared products exhibited good magnetic properties at room temperature.

## Experimental

### Materials and physical measurements

Magnesium chloride hexahydrate ( $\text{MgCl}_2 \cdot 6\text{H}_2\text{O}$ , Merck  $\geq 99\%$ ) ferric chloride hexahydrate ( $\text{FeCl}_3 \cdot 6\text{H}_2\text{O}$ , Merck  $\geq 99\%$ ) salts, sodium acetate trihydrate ( $\text{CH}_3\text{COONa} \cdot 3\text{H}_2\text{O}$ ,  $\geq 95\%$ ), Ethylene glycol (EG), PEG (Mn=4,000, Shanghai Chemical Reagent Co., Ltd., China) and were used for the synthesis of  $\text{MgFe}_2\text{O}_4$  nanoparticles. All chemicals were analytical grade and used as received without further purification. The X-ray diffraction (XRD) patterns of the  $\text{MgFe}_2\text{O}_4$  particles were obtained using an X'Pert PRO X-ray diffractometer (Model D8 Discover, Bruker) with  $\text{CuK}\alpha$  radiation ( $\lambda = 0.154 \text{ nm}$ ) in reflection mode and  $2\theta$  ranging from  $10^\circ$  to  $80^\circ$ . The morphological analysis of the samples is carried out using Scanning Electron Microscope (SEM, S-4700, Hitachi, Japan). The elemental composition of the samples is tested by energy-dispersive X-ray spectroscopy (EDX). Transmission electron microscopy (TEM) images were obtained on a Philips EM280 transmission electron microscopy with an accelerating voltage of 150 kV. The magnetic properties of the samples were measured with a vibrating sample magnetometer (VSM).  $\text{N}_2$  adsorption/ desorption isotherms were performed at  $196^\circ\text{C}$ , by a BELSORP mini-II surface area measurement equipment, after degassing the samples under vacuum at  $100^\circ\text{C}$  overnight. IR transmittance spectra of ferrite powder samples were measured on Bruker Equinox 55 infrared spectrophotometer (KBr pellets) in the range of  $4000\text{--}400\text{cm}^{-1}$ .

### Preparation of porous sphere-shaped $\text{MgFe}_2\text{O}_4$ particles

We synthesized porous magnesium ferrite ( $\text{MgFe}_2\text{O}_4$ ) nanospheres exactly in the same manner as described in our previous work [25] but with a small modification. In a typical preparation, firstly 2g of surfactant PEG was dissolved in 40 mL ethylene glycol under vigorous stirring to form a clear solution, and then 3.6 g sodium acetate trihydrate, 2.5 mmol  $\text{MgCl}_2 \cdot 6\text{H}_2\text{O}$  and 5 mmol  $\text{FeCl}_3 \cdot 6\text{H}_2\text{O}$  were added to the above solution. This mixture was

then vigorously stirred at  $50^\circ\text{C}$  for 30 min to form a homogeneous solution. Finally the mixture was transferred into a 100 mL Teflon-lined autoclave, which was heated at  $180^\circ\text{C}$  for 16 h. After being cooled to room temperature, the black powders were collected and washed several times with distilled water and ethanol to remove the impurities, and finally dried at  $80^\circ\text{C}$  in a vacuum oven for 8 h.

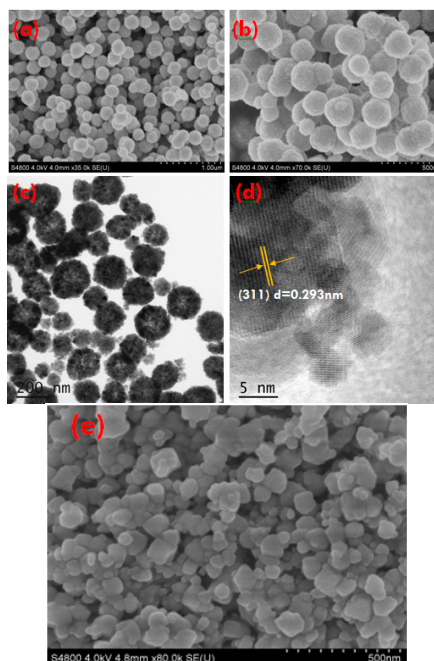
For comparison,  $\text{MgFe}_2\text{O}_4$  nanoparticles were also prepared using the same method without the introduction of PEG.

## Results and discussion

### Morphology and pore structures of $\text{MgFe}_2\text{O}_4$ nanospheres

Scanning electron microscope (SEM) was used to study the size and morphology of the porous sphere-like  $\text{MgFe}_2\text{O}_4$  particles and  $\text{MgFe}_2\text{O}_4$  nanoparticles (prepared without PEG). As shown in Figure. 1 (a&b), the micrographs indicate that they are 100–250 nm spheres in dimension and composed of small primary particles. The particles are packed tightly as an outcome of the attractive magnetic force and instinctive nature to reduce surface energy by aggregation. [26] TEM and HRTEM were used to further examine the morphology, particle size and crystallinity of the self-assembled products. Figure. 1c show TEM image of sphere-shaped  $\text{MgFe}_2\text{O}_4$  particles, it could be further observed that the products are formed by nanoparticles, which are consistent with the SEM images. As shown in Figure. 1c, sphere-shaped  $\text{MgFe}_2\text{O}_4$  nanoparticles are assembled by the layers of nanoparticles and exhibit porous structures at the center. Further evidence of the microstructure for sphere-shaped  $\text{MgFe}_2\text{O}_4$  particles is given in HRTEM image. HRTEM images shown in Figure. 1d confirmed the single-crystalline nature of the primary nanospheres. As depicted in Figure. 1d, the atomic lattice fringes can be clearly observed, and the interplanar spacings were measured to be 0.293 nm, which were close to the {311} lattice plane of cubic  $\text{MgFe}_2\text{O}_4$ . Figure. 1e shows the SEM image of  $\text{MgFe}_2\text{O}_4$  nanoparticles prepared without PEG for comparison.  $\text{MgFe}_2\text{O}_4$  nanoparticles are about 10–85 nm in diameter.

**Figure 1. SEM (a and b), TEM (c), HRTEM (d) images of  $\text{MgFe}_2\text{O}_4$  nanospheres and SEM (e) image of  $\text{MgFe}_2\text{O}_4$  nanoparticles**



Further, the nitrogen sorption measurement was conducted to evaluate the porous structure and specific surface area for such magnetic nanoparticles. Figure. 2 shows the large hysteresis loops between the adsorption and desorption isotherms in the P/P<sub>0</sub> ranging from 0.7 to 1, which confirms the formation of mesopore textural porosity and the slight pore size distribution towards smaller mesopores (see the inset of Figure. 2). The specific surface area was thus estimated, by Brunauer–Emmett–Teller (BET) equation [27], to be 53 m<sup>2</sup>/g. In addition, the sorption exhibits type IV isotherm and the pore analysis has revealed that the pore sizes in the porous nanospheres mainly fall into 7.59 nm, which are in good agreement with the TEM analysis. The generation of porosity is because of the interspace between nanoparticles; therefore, the pore size distribution is very broad. Moreover, such nanospheres possess a higher specific surface area than MgFe<sub>2</sub>O<sub>4</sub> nanoparticles.

### Crystal structure of the porous sphere-like MgFe<sub>2</sub>O<sub>4</sub> particles

Phase investigation of the crystallized products (porous sphere-like MgFe<sub>2</sub>O<sub>4</sub> particles and MgFe<sub>2</sub>O<sub>4</sub> nanoparticles) was performed by XRD and the diffraction pattern is presented in Figure. 3. All the XRD peaks can be indexed to the cubic spinel (JCPDS card no. 73-1960) structure with no extra lines corresponding to any other planes, which show that the prepared ferrites are single phase. The broadened nature of these diffraction peaks indicates that the grain size of the sample is on nano meter scale.

An additional quantitative analysis of the prepared porous MgFe<sub>2</sub>O<sub>4</sub> nanospheres was provided by EDX. EDX measurement results comply with what is expected from the synthesis. In other words, mass ratios of chemical compositions are in agreement with the outcomes of the EDX (Figure. 4). The experimental mass percentage and atom percentage for the sample are given in the Table (See Figure.4 inset).

### Magnetic properties of the porous sphere-like MgFe<sub>2</sub>O<sub>4</sub> particles

Such porous oriented ferrite nanospheres have exhibited good magnetic property. The hysteresis loop of the MgFe<sub>2</sub>O<sub>4</sub> spheres was recorded with VSM at the room temperature. The saturation magnetization (M<sub>s</sub>), remanent magnetization (M<sub>r</sub>) and coercivity

(H<sub>c</sub>) of the product were obtained based on the magnetic hysteresis loop. As shown in Figure. 5 and Table 1, the M<sub>s</sub>, M<sub>r</sub> and H<sub>c</sub> of nanospheres are 70.25 emu/g, 19.60 emu/g and 326.41 Oe respectively; for nanoparticles, they are 50.46 emu/g, 11.42 emu/g and 617.83 Oe. The saturation value of 70.25 emu/g obtained in the porous MgFe<sub>2</sub>O<sub>4</sub> nanospheres is higher than the value of 68.9 emu/g for MgFe<sub>2</sub>O<sub>4</sub> synthesized by a novel hydrothermal method [28] using acetates and aloe vera plant-extracted solution, 48.6 emu/g for MgFe<sub>2</sub>O<sub>4</sub> nanostructures fabricated by electrospinning [29], 30.6 emu/g for sol-gel/combustion synthesized MgFe<sub>2</sub>O<sub>4</sub> nano materials [30] and 14.09 emu/g for co-precipitation-synthesized MgFe<sub>2</sub>O<sub>4</sub> nanoparticles [31]. Porous sphere-like MgFe<sub>2</sub>O<sub>4</sub> nanospheres exhibit better magnetic properties than MgFe<sub>2</sub>O<sub>4</sub> nanoparticles.

According to the literature, the M<sub>s</sub>, M<sub>r</sub> and H<sub>c</sub> of the nanocrystals are merely determined by the size [32]. Moreover, the morphologies of MgFe<sub>2</sub>O<sub>4</sub> have some influence on magnetic properties [33]. Combined with XRD and TEM results, we suggest that the good magnetic properties of sphere-shaped MgFe<sub>2</sub>O<sub>4</sub> particles can be attributed to the high level of crystallinity and proper nanoparticle size, as well as the unique morphology.

FT-IR analysis was applied to investigate the presence of functional groups and impurity on the surface of the products. As can be seen in Figure. 6, The typical low frequency band at around 592 cm<sup>-1</sup> refers to Fe–O vibration (Fe<sup>3+</sup> bond) in octahedral and tetrahedral sites and the band at around 435 cm<sup>-1</sup> refers to Fe–O vibration (Fe<sup>2+</sup> bond) in octahedral sites [34]. In addition, the bands at 3411 and 1621 cm<sup>-1</sup> are attributed to the surface hydroxyl and the adsorbed water molecules, respectively [35]. The peak at 1078 cm<sup>-1</sup> may be attributed to the C–H bending frequencies of the remaining trace EG [36].

### Conclusions

In summary, we have successfully demonstrated a simple hydrothermal route to prepare porous MgFe<sub>2</sub>O<sub>4</sub> nanospheres. The most important advantage of this method is that it provides a one step, simple, general and inexpensive method for the preparation of ferrite nanoparticles at low synthesis temperature. The synthesized MgFe<sub>2</sub>O<sub>4</sub> nanoparticles had a spherical structure with a mean diameter of about 200 nm, higher surface area and high magnetization of 70.25 emu/g. These porous MgFe<sub>2</sub>O<sub>4</sub> nano

Figure 2. N<sub>2</sub> sorption isotherm of the porous MgFe<sub>2</sub>O<sub>4</sub> nanospheres, with insets showing the BJH pore-size distributions for the corresponding samples

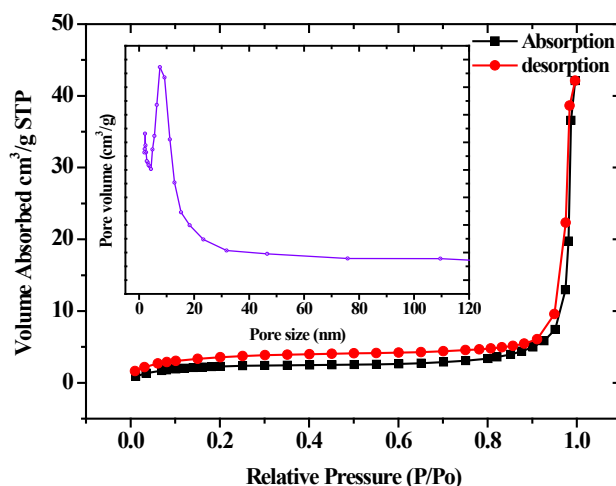


Figure 3. XRD patterns of the MgFe<sub>2</sub>O<sub>4</sub> nanoparticles (a) and porous MgFe<sub>2</sub>O<sub>4</sub> nanospheres (b)

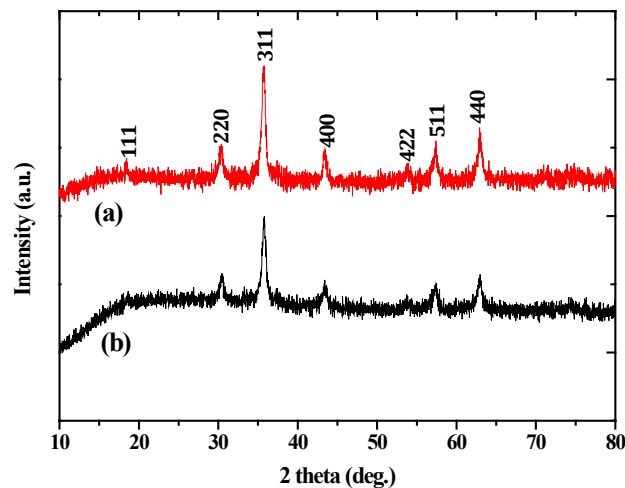


Figure 4. EDS spectrum for the porous MgFe<sub>2</sub>O<sub>4</sub> nanospheres

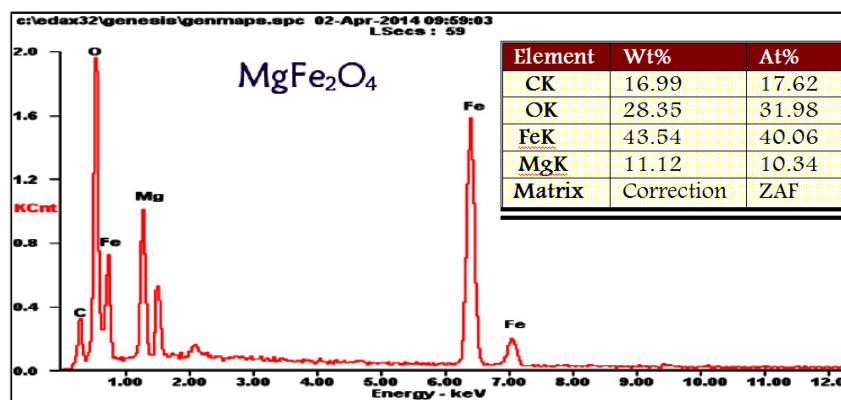


Table 1. Magnetic characteristic of the MgFe<sub>2</sub>O<sub>4</sub> nanoparticles

Sample	Ms (emu/g)	Mr (emu/g)	Hc (Oe)
MgFe <sub>2</sub> O <sub>4</sub> spheres	70.25	19.6	326.41
MgFe <sub>2</sub> O <sub>4</sub> particles	50.46	11.42	617.83

Figure 5. Magnetization hysteresis loop of the porous MgFe<sub>2</sub>O<sub>4</sub> nanospheres. The downright inset is an expanded low-field curve

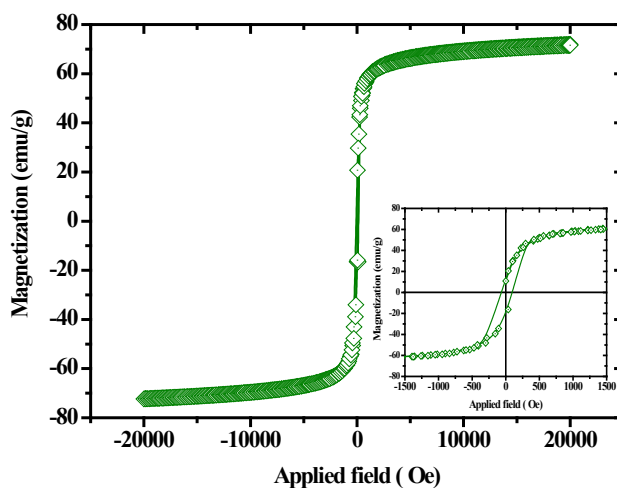
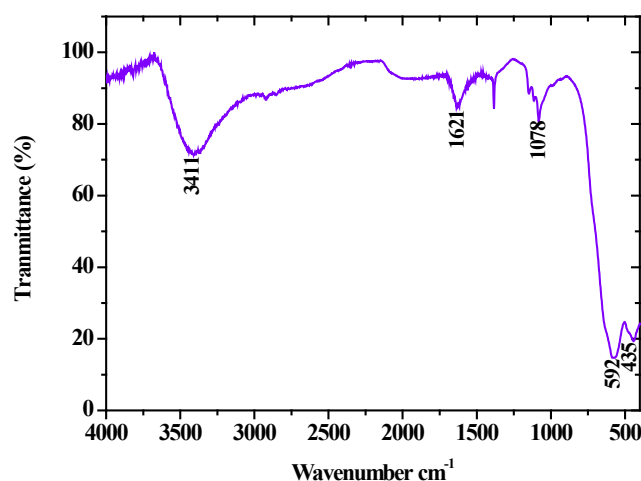


Figure 6. FTIR spectrum of the porous  $\text{MgFe}_2\text{O}_4$  nanospheres

spheres have excellent magnetic properties than that of the  $\text{MgFe}_2\text{O}_4$  nanoparticles. The developed magnetic nanomaterial is expected to find potential applications in separation, anodic material in lithium ion batteries, catalysts, and as electronic material for nanodevices and storage devices.

## Acknowledgement

Dr. Penchal Reddy Matli would like to acknowledge the financial supported by CAS fellowship For Postdoctoral and Visiting scholars from Developing Countries (Grant No. 2014FFGB0003).

## References

- [1]. R. C. O'Handley, (2000) *Modern Magnetic Materials: Principles and Applications*, Wiley & sons, New York.
- [2]. N. A. Spaldin, (2003) *Magnetic Materials: Fundamentals and Device Applications*, Cambridge University Press, Cambridge.
- [3]. Y.M. Huh, Y.W. Jun, H.T. Song, S. Kim, J.S. Choi, et al (2005) In vivo magnetic resonance detection of cancer by using multifunctional magnetic nanocrystals, *J. Am. Chem. Soc.* 127(35) 12387-97.
- [4]. H.T. Song, J.S. Choi, Y.M. Huh, S. Kim, Y.W. Jun, et al (2005) Surface Modulation of Magnetic Nanocrystals in the Development of Highly Efficient Magnetic Resonance Probes for Intracellular Labeling, *J. Amer. Chem. Soc.*, 127: 9992-9993
- [5]. K. An, T. Hyeon, (2009) Synthesis and biomedical applications of hollow nanostructures *Nano. Today* 4, 359-373.
- [6]. C.L. Jiang, Y.F. Wang, (2009) Formation of cobalt hollow nanospheres via surfactant-assisted hydrothermal progress, *Mater. Chem. Phys.* 113: 531.
- [7]. L.H. Lee, (2009) Gas sensors using hierarchical and hollow oxide nanostructures: Over view *Sens. Actuators B* 140: 319-336.
- [8]. C.J. Martinez, B. Hockey, C.B. Montgomery, S. Semancik, (2005) Porous tin oxide nano structured microspheres for sensor applications, *Langmuir* 21(17): 7937-44.
- [9]. Y. Shen, Y. Wu, X. Li, Q. Zhao, Y. Hou, (2013) One-Pot Synthesis Of  $\text{MgFe}_2\text{O}_4$  Nanospheres By Solvothermal Method, *Mater. Lett.* 96: 85.
- [10]. J.n. Dui, G.y. Zhu, S.m. Zhou, (2013) Facile And Economical Synthesis Of Large Hollow Ferrites And Their Applications In Adsorption For As(V) And Cr(VI). *ACS Appl. Mater. Interfaces* 5(20): 10081- 10089.
- [11]. M. Fu, Q. Z. Jiao, Y. Zhao, (2013) Preparation of  $\text{NiFe}_2\text{O}_4$  nanorod - raphene composites VIA an ionic liquidassisted one-step hydrothermal approach and their microwave absorbing properties, *J. Mater. Chem. A.* 1: 5577-5586.
- [12]. Q. Liu, H.X. Huang, L.F. Lai, (2009) Hydrothermal synthesis and magnetic properties of  $\text{NiFe}_2\text{O}_4$  nanoparticles and nanorods. *J. Mater. Sci.* 44(5): 1187-1191.
- [13]. J. Fu, J. Zhang, Y. Peng, (2013) Wire-in-tube structure fabricated by single capillary electrospinning via nanoscale Kirkendall effect: the case of nickel-zinc ferrite. *Nanoscale*, 5(24):12551.
- [14]. Q.I. Li, C.b. Chang, H.x. Jing, Y.f. Wang. J. (2010) Synthesis And Characterization Of Shape-Controlled  $\text{Ni}_0.5\text{zn}_0.5\text{Fe}_2\text{O}_4$  via The Coprecipitation Method. *Alloys Compd.* 49: 6-66.
- [15]. C.P. Huu, N. Keller, C. Estournes, G. Ehret, M. Ledoux, (2002) Synthesis of  $\text{CoFe}_2\text{O}_4$  nanowire in carbon nanotubes. A new use of the confinement effect. *Chem. Commun.* 17: 1882-1883.
- [16]. C.P. Huu, N. Keller, C. Estournes, G. Ehret, J. Greneche, et al, (2003) Microstructural investigation and magnetic properties of  $\text{CoFe}_2\text{O}_4$  nanowires synthesized inside carbon nanotubes. *Phys. Chem. Chem. Phys.* 5: 3716-3723.
- [17]. Y. Sun, G. Ji, M. Zheng, X. Chang, S. Li, et al, (2010) Synthesis and magnetic properties of crystalline mesoporous  $\text{CoFe}_2\text{O}_4$  with large specific surface area. *J. Mater. Chem.* 20: 945-952.
- [18]. Z. Gao, F. Cui, S. Zeng, L. Guo, J. Shi, (2010) Microporous Mesoporous Mater. 132: 188.
- [19]. R.J. WILLEY, P. NOIRCLERC, G. BUSCA, (1993) PREPARATION AND CHARACTERIZATION OF MAGNESIUM CHROMITE AND MAGNESIUM FERRITE AEROGELS. *CHEM. ENG. COMMUN.* 123: 1-16.
- [20]. Y.L. Liu, Z.M. Liu, Y. Yang, H.F. Yang, G.L. R.Q. Shen, (2005) Simple synthesis of  $\text{MgFe}_2\text{O}_4$  nanoparticles as gas sensing materials. *Sens Actuators B.* 107:600-104.
- [21]. D. Chen, Y.Z. Zhang, C.J. Tu, (2012) Preparation of high saturation magnetic  $\text{MgFe}_2\text{O}_4$  nanoparticles by microwave-assisted ball milling. *Mater. Lett.* 82: 10-12.
- [22]. H.G. Kim, P.H. Borse, J.S. Jang, E.D. Jeong, O.S. Jung, et al, (2009) Fabrication of  $\text{CaFe}_2\text{O}_4/\text{MgFe}_2\text{O}_4$  bulk heterojunction for enhanced visible light photocatalysis. *Chem. Commun.* 5889-5891.
- [23]. R.K. Gupta, F. Yakuphanoglu, (2011) Epitaxial growth of  $\text{MgFe}_2\text{O}_4$  (111) thin films on sapphire (0001) substrate. *Mater. Lett.* 65: 3058-3060.
- [24]. W.Q. Meng, F. Li, D.G. Evans, X. Duan, (2004) Preparation of magnetic material containing  $\text{MgFe}_2\text{O}_4$  spinel ferrite from a Mg-Fe(III) layered double hydroxide intercalated by hexacyanoferrate(III) ions. *Mater. Chem. Phys.* 86:1-4.
- [25]. M. Penchal Reddy, X. Zhou, D. Shiyu, Q. Huang, (2014) *Inter. Nano. Lett.* (Article In Press)
- [26]. S.B. Ni, X.L. Sun, X.H. Wang, G. Zhou, F. Yang, J.M. Wang, D.Y. He, Low temperature synthesis of  $\text{Fe}_3\text{O}_4$  micro-spheres and its microwave absorption properties. *Mater. Chem. Phys.* 124: 353-358.
- [27]. S. Brunauer, P.H. Emmett, E. Teller, (1938) Adsorption of Gases in Multimolecular Layers. *J. Am. Chem. Soc.* 60: 309-319.
- [28]. S. Phumying, S. Labuayai, E. Swatsitang, V. Amornkitbamrung, S. Maensiri, (2013) Nanocrystalline spinel ferrite ( $\text{MFe}_2\text{O}_4$ , M = Ni, Co, Mn, Mg, Zn) powders prepared by a simple aloe vera plant-extracted solution hydrothermal route. *Mater. Res. Bull.* 48: 2060-2065.
- [29]. S. Maensiri, M. Sangmanee, A. Wiengmoon, (2009) Magnesium Ferrite ( $\text{MgFe}_2\text{O}_4$ ) Nanostructures Fabricated by Electrospinning. *Nanoscale Res. Lett.* 4:221-228.
- [30]. Y. Huang, Y. Tang, J. Wang, Q. Chen, (2006) Synthesis of  $\text{MgFe}_2\text{O}_4$  nanocrystallites under mild conditions. *Mater. Chem. Phys.* 97: 394-397.
- [31]. M.M. Rashad, (2007) Magnetic properties of nanocrystalline magnesium ferrite by co-precipitation assisted with ultrasound irradiation. *J. Mater. Sci.* 42:5248.
- [32]. Q. Song, Z.J. Zhang, (2004) Shape Control and Associated Magnetic Properties of Spinel Cobalt Ferrite Nanocrystals. *J. Am. Chem. Soc.* 126: 6164-6168.
- [33]. M. Ozaki, H. Suzuki, K. Takahashi, E. Matijevic, (1986) Reversible ordered agglomeration of hematite particles due to weak magnetic interactions. *J.*

- Colloid. Interface Sci.113: 76-80.
- [34]. J. Mohapatra, A. Mitra, D. Bahadur, M. Aslam, (2013) Surface controlled synthesis of  $MFe_2O_4$  ( $M = Mn, Fe, Co, Ni$  and  $Zn$ ) nanoparticles and their magnetic characteristics. *Crystengcomm.* 15: 524-532.
- [35]. X.F. Song, L. Gao, (2007) Synthesis, Characterization, and Optical Properties of Well-Defined N-Doped, Hollow Silica/Titania Hybrid Microspheres. *Langmuir.* 23:11850-11856.
- [36]. B. Baruwati, M.N. Nadagouda, R.S. Varma, (2008) Bulk Synthesis of Monodisperse Ferrite Nanoparticles at Water–Organic Interfaces under Conventional and Microwave Hydrothermal Treatment and Their Surface Functionalization, *J. Phys. Chem.C.* 112:18399-18404.